

Opti521 Engineering Memorandum

TITLE: Synopsis of Technical Paper: "Determination of the dihedral angle errors of a corner cube from its Twyman-Green interferogram"			EM Number: Opti-521 - Synopsis-1 Date 10-Nov-06 Revised: Version:
AUTHOR(S): Larry Burriesci	PHONE: (650) 424-2213	ORGN: LMATC	APPROVALS: Prof. Jim Burge

page 1 of 5 pages

I have chosen a paper by D.A. Thomas and J.C. Wyant from 1976 that presents the theory and implementation of a method for measuring the errors in the as-built dihedral angle errors of corner cube reflectors.

Determination of the dihedral angle errors of a corner cube from its Twyman-Green interferogram

David A. Thomas and J. C. Wyant
Optical Sciences Center, University of Arizona, Tucson, Arizona 85721
(Received 20 September 1976)
J. Opt. Soc. Am., Vol. 67, No. 4, April 1977

A technique is devised for calculating the magnitudes of the dihedral angle errors of a corner cube from a single Twyman-Green interferogram. Experimental examples are given in which the dihedral angles of two corner cubes are determined to within 2 arcsec by this procedure. These values are shown to be in good agreement with independent goniometer measurements.

The key results reported in the paper are these five:

- (1) This method allows the calculation of the magnitudes of the errors in the dihedral angles from a single Twyman-Green interferogram.
- (2) Such interferograms are routinely supplied by manufacturers as evidence of the quality of their product.
- (3) When a perfect cube is tested in this fashion, the prism aperture is covered by a single sinusoidal fringe pattern. Imperfect prisms with planar reflecting surf sinusoidal fringe patterns over their apertures. The patterns are usually inclined at various angles with respect to one another, and each one generally has a different spatial frequency. When the prism is illuminated with a plane wave, a component plane wave will emerge from each of these segments. It is the interference between these emerging beams and a common reference plane wave that gives the fringe patterns.
- (4) This method employs the same vector matrix approach used in an earlier work by P.R. Yoder, Jr. from 1958 when laser interferometry was not used, but a pinhole illuminator and readout as "dot patterns". Yoder's method had to rely on independent measurements of the dihedral angles on a goniometer for the input values of his calculations.
- (5) Intermediate work in 1972 by Joseph and Donohue used the dot pattern data to compute the relative sign and magnitude of all three dihedral angle errors.

Usefulness and Applications:

This information is useful to someone who needs to understand how to employ the theory and practice involved in characterizing prism errors. It is a template paper that can serve to baseline associated work in designing a measurement program for similar optical elements. Because the paper provides good connections to other related work, it allows the reader to research some good options through comparing and contrasting them.

Relationship between this paper and other similar papers:

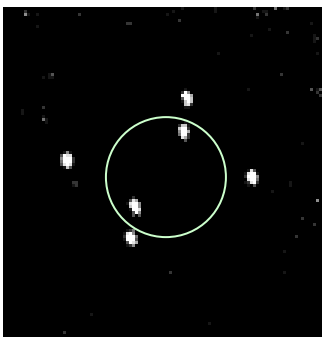
Yoder P. R. Yoder, Jr., "Study of the light deviation errors in triple mirrors and tetrahedral prisms," J. Opt. Soc. Am. 48, 496-499 (1958).: Defines the theoretical approach and codifies the mathematical analysis for determining the dihedral angle errors; also demonstrates "dot pattern" tests; uses a pinhole, a light bulb and an optical autocollimator.

Joseph and Donohue B. W. Joseph and R. J. Donohue, "Dot patterns from imperfect angle. cube-corner reflections," J. Opt. Soc. Am. 62, 727 (A) (1972).: used the pattern data to compute the relative sign and magnitude of all three dihedral angle errors.

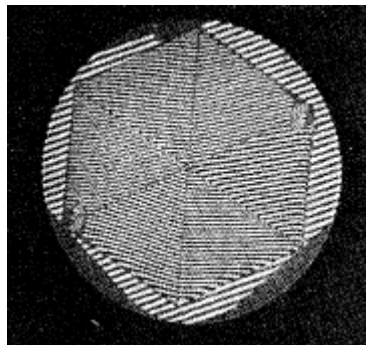
Thomas and Wyant A. Thomas and J. C. Wyant, "Determination of the dihedral angle errors of a corner cube from its Twyman-Green interferogram," J. Opt. Soc. Am. 67, 467-472 (1977).: Adds T-G laser interferogram analysis to characterize dihedral angle error magnitudes; uses Yoder's vector analysis mathematics and labeling conventions for dihedral surfaces.

Ai and Smith Chiayu Ai and Kenneth L. Smith "Accurate measurement of the dihedral angle of a corner cube" APPLIED OPTICS 1 February 1992 / Vol. 31, No. 4 / : Extends the analysis to tilted corner cubes; also employs Yoder's math and labeling.

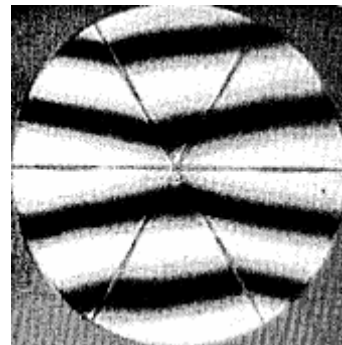
Scholl, Marija S. Scholl "Ray trace through a corner-cube retroreflector with complex reflection coefficients" J. Opt. Soc. Am. A Vol. 12, No. 7/ July 1995/: Extends the analysis to include complex coefficients of reflectivity and phase conjugation.



**Yoder, 1958
(dot pattern with
specification circle)**



Thomas and Wyant, 1976



Ai and Smith, 1992

Synopsis:

When the Thomas and Wyant paper was submitted for publication in 1976, several authors had already used the dot patterns produced by the reflection of a pencil of light from imperfect corner cubes to quantify their imperfections. P. R. Yoder, Jr. developed relationships that gave the deviation angles of the emerging beams with respect to the illuminating beam as a function of the three dihedral angle errors for the cube. Yoder was able to favorably compare his calculated deviation angle values to the figures

obtained directly from the dot patterns, but he had to rely on independent measurements of the dihedral angles for the input values of his calculations.

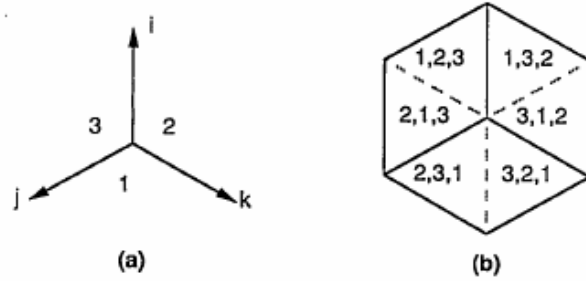


Fig. 1. (a) Corner cube coordinates and reflections.³ (b) Prism apertures with the associated reflection sequence.

Yoder's conventions

In this article by Thomas and Wyant, the authors first draw several parallels to the previous works on characterization of errors in the dihedral angles, and then they extend the discussion to characterization using Twyman-Green interferograms. In their first section on theoretical development the propagation vectors for six distinct emergent beams are baselined. Very importantly, Yoder's system of grouping the vectors into pairs is presented in which a pair is defined as those two emergent beams that share a common face for their third and final reflection. In this manner of grouping, each corner cube dihedral angle error can be isolated by comparing the fringe patterns in one of these three pairs of aperture segments.

Thomas and Wyant next present combinatorial relationships for the corner cube faces by successively applying the vector law of reflection, where they reference MIL-HDBK-141, pages 13-1 through 13-9 on mirror and prism system reflection vector matrices. The vector law of reflection is written as:

$$\mathbf{S}_1 = \mathbf{S}_0 - 2(\mathbf{S}_0 \cdot \mathbf{M})\mathbf{M}$$

where \mathbf{S}_0 is the unit propagation vector for the incident beam, \mathbf{S}_1 the unit propagation vector for the reflected beam, and \mathbf{M} the outward pointing unit normal to the reflecting surface.

Examples are given to show that a three-by-three reflection matrix $[\mathbf{R}]$ characteristic of the reflector can be used to map an incident ray into its conjugate reflected ray

$$\begin{pmatrix} S_{1x} \\ S_{1y} \\ S_{1z} \end{pmatrix} = \begin{pmatrix} (1 - 2 M_x^2) & -2 M_x M_y & -2 M_x M_z \\ -2 M_x M_y & (1 - 2 M_y^2) & -2 M_x M_z \\ -2 M_x M_z & -2 M_y M_z & (1 - 2 M_z^2) \end{pmatrix} \begin{pmatrix} S_{0x} \\ S_{0y} \\ S_{0z} \end{pmatrix} \quad [1]$$

For a series of three reflections,

$$(\mathbf{S}')_{ijk} = (\mathbf{R})_k (\mathbf{R})_j (\mathbf{R})_i (\mathbf{S}_0) = (\mathbf{R})_{ijk} (\mathbf{S}_0) \quad [2]$$

where $i, j, k = 1, 2, 3$ and $i \neq j \neq k$

Once the direction cosines of the unit normals to the three reflecting surfaces of a corner cube are known, system reflection matrices can be calculated for each of the six possible sequences of reflections that can be used to map the illuminating ray into each of the final exiting rays.

Next, it is postulated that if the errors in the dihedral angles are small, they can be written as $(\pi/2 + \varepsilon)$, and that if the angle between a pair of surface normals is θ , then $\cos \theta = \sin \varepsilon$. Then, one can write the various values for θ as:

$$\begin{aligned}\cos \theta_{12} &= M_{1x} M_{2x} + M_{1y} M_{2y} + M_{1z} M_{2z} = \sin \varepsilon_{12} \\ \cos \theta_{13} &= M_{1x} M_{3x} + M_{1y} M_{3y} + M_{1z} M_{3z} = \sin \varepsilon_{13} \\ \cos \theta_{23} &= M_{2x} M_{3x} + M_{2y} M_{3y} + M_{2z} M_{3z} = \sin \varepsilon_{23}\end{aligned}\quad [3]$$

Thomas and Wyant then adopt the same specific orientation for the corner cube with respect to Cartesian coordinate axes originally introduced by Yoder in the referenced 1958 paper. Namely, let M_1 coincide with the i-direction and let the dihedral edge between surfaces 1 and 2 be parallel to the k-direction. Since the surface normals must have unit length, the M values become:

$$\begin{aligned}M_{1x} &= 1, & M_{2x} &= \sin \varepsilon_{12}, & M_{3x} &= \sin \varepsilon_{13}, \\ M_{1y} &= 0, & M_{2y} &= \cos \varepsilon_{12} & M_{3y} &= (\sin \varepsilon_{23} - \sin \varepsilon_{12} \sin \varepsilon_{13}) / \cos \varepsilon_{12}, \\ M_{1z} &= 0, & M_{2z} &= 0 & M_{3z} &= (1 - M_{3x}^2 - M_{3y}^2)^{1/2}\end{aligned}\quad [4]$$

To a first-order small angle approximation, $\cos \varepsilon = 1$ and $\sin \varepsilon = \varepsilon$, a familiar rule of thumb used in simplification of reflection matrices. The surface normal coordinates then reduce to:

$$\begin{aligned}M_{1x} &= 1, & M_{2x} &= \varepsilon_{12}, & M_{3x} &= \varepsilon_{13}, \\ M_{1y} &= 0, & M_{2y} &= 1, & M_{3y} &= \varepsilon_{23}, \\ M_{1z} &= 0, & M_{2z} &= 0, & M_{3z} &= 1\end{aligned}\quad [5]$$

By substituting these surface normal coordinates into the example reflection matrix of equation [1], the resulting reflection matrices become:

$$[\mathbf{R}]_1 = \begin{pmatrix} -1 & 0 & 0 \\ 0 & 1 & 0 \\ 0 & 0 & 1 \end{pmatrix}; \quad [\mathbf{R}]_2 = \begin{pmatrix} 1 & -2\varepsilon_{12} & 0 \\ -2\varepsilon_{12} & -1 & 0 \\ 0 & 0 & 1 \end{pmatrix}; \quad [\mathbf{R}]_3 = \begin{pmatrix} 1 & 0 & -2\varepsilon_{13} \\ 0 & 1 & -2\varepsilon_{23} \\ -2\varepsilon_{13} & -2\varepsilon_{23} & -1 \end{pmatrix}\quad [6]$$

The system reflection matrix for each of the six possible sequences of corner cube reflections can now be obtained by multiplying these three reflection matrices together in the appropriate order. For example:

$$\begin{aligned}[\mathbf{R}]_{123} &= \begin{pmatrix} -1 & -2\varepsilon_{12} & -2\varepsilon_{13} \\ 2\varepsilon_{12} & -1 & -2\varepsilon_{23} \\ 2\varepsilon_{13} & 2\varepsilon_{23} & -1 \end{pmatrix}; \quad [\mathbf{R}]_{132} = \begin{pmatrix} -1 & -2\varepsilon_{12} & -2\varepsilon_{13} \\ 2\varepsilon_{12} & -1 & -2\varepsilon_{23} \\ 2\varepsilon_{13} & 2\varepsilon_{23} & -1 \end{pmatrix}; \\ [\mathbf{R}]_{231} &= \begin{pmatrix} -1 & 2\varepsilon_{12} & 2\varepsilon_{13} \\ -2\varepsilon_{12} & -1 & -2\varepsilon_{23} \\ -2\varepsilon_{13} & 2\varepsilon_{23} & -1 \end{pmatrix}; \quad [\mathbf{R}]_{312} = \begin{pmatrix} -1 & -2\varepsilon_{12} & 2\varepsilon_{13} \\ 2\varepsilon_{12} & -1 & 2\varepsilon_{23} \\ -2\varepsilon_{13} & -2\varepsilon_{23} & -1 \end{pmatrix}\end{aligned}\quad [7]$$

The remaining reflection sequences are the reverse of the three sequences just listed as examples.

Their system reflection matrices may be obtained from the corresponding forward sequence matrices above by reversing the signs on the matrix elements in the upper right and lower left quadrants while leaving the main diagonal elements unchanged. Once an illuminating beam is specified, one can find the reflected beam vectors $[S]_{ijk}$ for the corner cube by substituting each of the six system reflection matrices into equation [2]. The prism is typically illuminated along its nominal axis of symmetry so that the aperture segments will have the same apparent size in the resulting interferogram. The direction cosines in this case are all equal to $(3)^{1/2}/3 = 0.577$, and the corresponding $[S]_{ijk}$ components are:

$$\begin{aligned}
 [S']_{\mathbf{x}_{123}} &= -\frac{\sqrt{3}}{3(1+2\epsilon_{12}+2\epsilon_{13})} \mathbf{i} & [S']_{\mathbf{x}_{213}} &= -\frac{\sqrt{3}}{3(1+2\epsilon_{13}-2\epsilon_{12})} \mathbf{i} \\
 [S']_{\mathbf{y}_{123}} &= -\frac{\sqrt{3}}{3(1+2\epsilon_{23}-2\epsilon_{12})} \mathbf{j} & [S']_{\mathbf{y}_{213}} &= -\frac{\sqrt{3}}{3(1+2\epsilon_{12}+2\epsilon_{23})} \mathbf{j} \\
 [S']_{\mathbf{z}_{123}} &= -\frac{\sqrt{3}}{3(1-2\epsilon_{13}-2\epsilon_{23})} \mathbf{k} & [S']_{\mathbf{z}_{213}} &= -\frac{\sqrt{3}}{3(1-2\epsilon_{13}-2\epsilon_{23})} \mathbf{k}
 \end{aligned} \tag{8}$$

and so on ...

The six beams that emerge from the corner cube are interfered with a common reference beam to obtain a Twyman-Green interferogram. The cross product between reference beam and emergent beam not only points in the direction that the fringes resulting from the interference of these two beams would have, but also has a magnitude equal to the sine of the angle between the two vectors. This magnitude is also equal to the wavelength of light times the spatial frequency of the fringes.

Thomas and Wyant de-convolve the completed set of error contributions into the net dihedral angle errors $\delta_1, \delta_2, \delta_3$ associated with surfaces 1,2,3 to arrive at the result:

$$(\delta_1 + \delta_2 + \delta_3) = (3)^{1/2}/2(\lambda F)^2,$$

where F is the spatial frequency of the fringes that would be observed with a perfect corner cube. The fringe patterns associated with imperfect cubes will have spatial frequencies of the same order of magnitude as F since the various emergent beams make small angles with the illuminating beam in such cases provided the dihedral angle errors are small.

The fringes that are recorded in a Twyman-Green interferogram are the projections of the actual fringes onto a plane that is nearly normal to the beam used to illuminate the corner cube. If the results obtained by the technique just described are to be accurate, we must be sure that the actual fringe vectors always lie sufficiently close to the interferogram plane to neglect their deviation from that plane.

Finally, it should be noted that the ϵ_{ij} values calculated by the above technique should be divided by the refractive index to obtain the actual values when a glass prism is being tested interferometrically to compensate for refraction at the air-glass interface at the front of the corner cube.

of $u(\mathbf{r})$ the field $v(\mathbf{r}) = u(\mathbf{r}) - \langle u(\mathbf{r}) \rangle$ which, of course, satisfies the constraint $\langle v(\mathbf{r}) \rangle = 0$.

⁵In the phenomenological theory equations (2.8) and (2.9) are assumed to hold generally, Eq. (2.10) is assumed to hold only in free space. For fields interacting with matter Eq. (2.10) is replaced by a more general equation of radiative transfer. [See, for example, S. Chandrasekhar, *Radiative Transfer* (Dover, New York, 1960), Secs. 2.2, 2.3, and 6.].

⁶L. S. Dolin, "Beam Description of Weakly-Inhomogeneous Wave Fields," *Izv. vuzov (Radiofizika)* 7, 559 (1964).

⁷See, for example, J. D. Jackson, *Classical Electrodynamics*, 2nd ed. (Wiley, New York, 1975), Eq. (3.61), p. 100. We have omitted in (3.6) terms of the form $B_{lm}(\mathbf{s})R^{-(l+1)}Y_{lm}(\theta, \phi)$,

since they are singular when $R = 0$.

⁸V. I. Tatarski, *Wave Propagation in a Turbulent Medium* (McGraw-Hill, New York, 1961; reproduced by Dover, New York, 1967).

⁹G. I. Ovchinnikov and V. I. Tatarskii, "On the Problem of the Relationship between Coherence Theory and the Radiation-Transfer Equation," *Radiophys. Quant. Electron.* 15, 1087 (1972).

¹⁰E. Wolf, "New theory of radiative energy transfer in free electromagnetic fields," *Phys. Rev. D*, 13, 869 (1976).

¹¹See also M. S. Zubairy and E. Wolf, "Exact Equations for Radiative Transfer of Energy and Momentum in Free Electromagnetic Fields," *Optics Commun.* (in press).

Determination of the dihedral angle errors of a corner cube from its Twyman-Green interferogram

David A. Thomas and J. C. Wyant

Optical Sciences Center, University of Arizona, Tucson, Arizona 85721

(Received 20 September 1976)

A technique is devised for calculating the magnitudes of the dihedral angle errors of a corner cube from a single Twyman-Green interferogram. Experimental examples are given in which the dihedral angles of two corner cubes are determined to within 2 arcsec by this procedure. These values are also shown to be in good agreement with independent goniometer measurements.

INTRODUCTION

Several authors have used the dot patterns produced by the reflection of a pencil of light from imperfect corner cubes to quantify their imperfections. Yoder¹ developed relationships that gave the deviation angles of the emerging beams with respect to the illuminating beam as a function of the three dihedral angle errors for the cube. He was able to favorably compare his calculated deviation angle values to the figures obtained directly from the dot patterns, but had to rely on independent measurements of the dihedral errors for the input values of his calculations. Joseph and Donohue² used the pattern data to compute the relative sign and magnitude of all three dihedral angle errors.

Corner cubes can also be readily tested with a Twyman-Green interferometer. Such interferograms are, in fact, often supplied by manufacturers as evidence of the quality of their product. When a perfect cube is tested in this fashion, the prism aperture is covered by a single sinusoidal fringe pattern. Imperfect prisms with planar reflecting surfaces generally have six distinct sinusoidal fringe patterns over their apertures. The patterns are usually inclined at various angles with respect to one another, and each one generally has a different spatial frequency. This paper describes the use of such an interferogram to determine the magnitudes of the dihedral angle errors of a corner cube. The derivation follows Yoder's basic matrix algebra approach.

THEORETICAL DEVELOPMENT

When a corner cube is viewed along its nominal axis of symmetry, its aperture is seen to be divided into six

equal triangular segments. When the prism is illuminated with a plane wave, a component plane wave will emerge from each of these segments. It is the interference between these emerging beams and a common reference plane wave that gives the fringe patterns mentioned in the introduction. An incident ray must undergo a sequence of three reflections in passing through the prism, and each of the six possible reflection sequences is associated with one of the aperture segments. If the three prism faces are numbered in a counterclockwise sequence starting with the lower face, the aperture segments would be associated with the reflection sequences indicated in Fig. 1. It is important to note that these segments can be grouped in pairs such that each member of a pair has a common face for its final reflection. This fact suggests that each corner cube dihedral angle error can be isolated by comparing the fringe patterns in one of these three pairs of aperture segments.

Since the angular orientations and spatial frequencies of the fringe patterns being examined depend on the angular relationships between the interfering beams, the theoretical treatment must be vectorial in nature. The propagation vectors for the six beams that emerge from a corner cube when it is illuminated by a single plane wave can be obtained by successively applying the vector law of reflection to the three reflecting surfaces. This law is derived in one of the references³ and can be written

$$\mathbf{S}_1 = \mathbf{S}_0 - 2(\mathbf{S}_0 \cdot \mathbf{M})\mathbf{M}, \quad (1)$$

where \mathbf{S}_0 is the unit propagation vector for the incident beam, \mathbf{S}_1 the unit propagation vector for the reflected beam, and \mathbf{M} the outward pointing unit normal to the

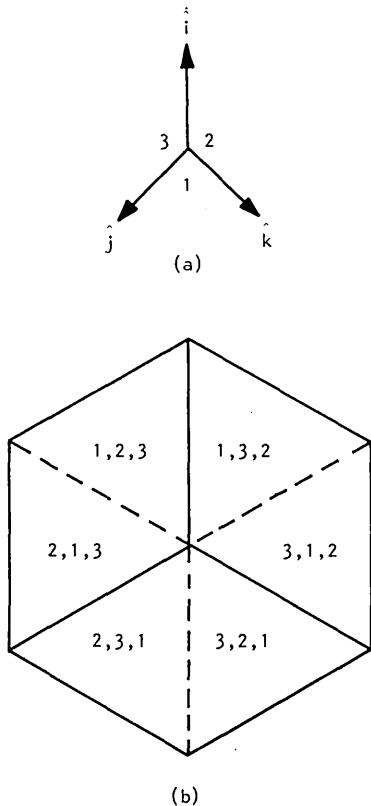


FIG. 1. Corner cube reflections. (a) Coordinate system and numbering sequence for reflecting surfaces. (b) Prism aperture with associated reflection sequences.

reflecting surface. This vector equation may be re-written in matrix form as

$$\begin{bmatrix} S_{1x} \\ S_{1y} \\ S_{1z} \end{bmatrix} = \begin{bmatrix} (1 - 2M_x^2) & -2M_xM_y & -2M_xM_z \\ -2M_xM_y & (1 - 2M_y^2) & -2M_yM_z \\ -2M_xM_z & -2M_yM_z & (1 - 2M_z^2) \end{bmatrix} \begin{bmatrix} S_{0x} \\ S_{0y} \\ S_{0z} \end{bmatrix}. \quad (2)$$

In this form the equation shows that a three-by-three reflection matrix $[R]$ characteristic of the reflector can be used to map an incident ray into its conjugate reflected ray. For a series of three reflections, we have

$$[S]_{ijk}^1 = [R]_k [R]_j [R]_i [S]_0, \quad (3)$$

or

$$[S]_{ijk}^1 = [R]_{ijk} [S]_0, \quad (4)$$

where $i, j, k = 1, 2, 3$ and $i \neq j \neq k$. Once the direction cosines of the unit normals to the three reflecting surfaces of a corner cube are known, system reflection matrices can be calculated for each of the six possible sequences of reflections that can be used to map the illuminating ray into each of the final exciting rays.

If we assume that the dihedral angles are only slightly in error, we can write them as $(\pi/2 + \epsilon)$. If we also designate the angle between a pair of surface normals by θ , then $\cos\theta = \sin\epsilon$, and we can now write the various values of θ as

$$\cos\theta_{12} = M_{1x}M_{2x} + M_{1y}M_{2y} + M_{1z}M_{2z} = \sin\epsilon_{12},$$

$$\cos\theta_{13} = M_{1x}M_{3x} + M_{1y}M_{3y} + M_{1z}M_{3z} = \sin\epsilon_{13}, \quad (5)$$

$$\cos\theta_{23} = M_{2x}M_{3x} + M_{2y}M_{3y} + M_{2z}M_{3z} = \sin\epsilon_{23}.$$

The prism must now be given a specific orientation with respect to the Cartesian coordinate axes in order to specify the components of the three surface normals. We assume for computational convenience and without loss of generality that M_1 coincides with \hat{i} and that the dihedral edge between surfaces 1 and 2 is parallel to \hat{k} . This scheme was originally introduced by Yoder and can be used in conjunction with the fact that the surface normals must have unit length to show that

$$\begin{aligned} M_{1x} &= 1, & M_{2x} &= \sin\epsilon_{12}, & M_{3x} &= \sin\epsilon_{13}, \\ M_{1y} &= 0, & M_{2y} &= \cos\epsilon_{12}, & M_{3y} &= (\sin\epsilon_{23} - \sin\epsilon_{12}\sin\epsilon_{13})/\cos\epsilon_{12}, \\ M_{1z} &= 0, & M_{2z} &= 0, & M_{3z} &= (1 - M_{3x}^2 - M_{3y}^2)^{1/2}. \end{aligned} \quad (6)$$

To a first-order small angle approximation, $\cos\epsilon = 1$ and $\sin\epsilon = \epsilon$, and the surface normal coordinates reduce to

$$\begin{aligned} M_{1x} &= 1, & M_{2x} &= \epsilon_{12}, & M_{3x} &= \epsilon_{13}, \\ M_{1y} &= 0, & M_{2y} &= 1, & M_{3y} &= \epsilon_{23}, \\ M_{1z} &= 0, & M_{2z} &= 0, & M_{3z} &= 1. \end{aligned} \quad (7)$$

By substituting these coordinates into the reflection matrix given in Eq. (2), the reflection matrices obtained for the three corner cube faces are

$$\begin{aligned} [R]_1 &= \begin{bmatrix} -1 & 0 & 0 \\ 0 & 1 & 0 \\ 0 & 0 & 1 \end{bmatrix}, \\ [R]_2 &= \begin{bmatrix} 1 & -2\epsilon_{12} & 0 \\ -2\epsilon_{12} & -1 & 0 \\ 0 & 0 & 1 \end{bmatrix}, \\ [R]_3 &= \begin{bmatrix} 1 & 0 & -2\epsilon_{13} \\ 0 & 1 & -2\epsilon_{23} \\ -2\epsilon_{13} & -2\epsilon_{23} & -1 \end{bmatrix}. \end{aligned} \quad (8)$$

The system reflection matrix for each of the six possible sequences of corner cube reflections can now be obtained by multiplying the component matrices given in Eq. (8) in the appropriate order. For example,

$$\begin{aligned} [R]_{123} &= \begin{bmatrix} 1 & 0 & -2\epsilon_{13} \\ 0 & 1 & -2\epsilon_{23} \\ -2\epsilon_{13} & -2\epsilon_{23} & -1 \end{bmatrix} \\ &\times \begin{bmatrix} 1 & -2\epsilon_{12} & 0 \\ -2\epsilon_{12} & -1 & 0 \\ 0 & 0 & 1 \end{bmatrix} \begin{bmatrix} -1 & 0 & 0 \\ 0 & 1 & 0 \\ 0 & 0 & 1 \end{bmatrix}, \end{aligned} \quad (9)$$

or

$$[R]_{123} = \begin{bmatrix} -1 & -2\epsilon_{12} & -2\epsilon_{13} \\ 2\epsilon_{12} & -1 & -2\epsilon_{23} \\ 2\epsilon_{13} & 2\epsilon_{23} & -1 \end{bmatrix} . \quad (10)$$

Similarly,

$$[R]_{231} = \begin{bmatrix} -1 & 2\epsilon_{12} & 2\epsilon_{13} \\ -2\epsilon_{12} & -1 & -2\epsilon_{23} \\ -2\epsilon_{13} & 2\epsilon_{23} & -1 \end{bmatrix} \text{ and} \quad (11)$$

$$[R]_{312} = \begin{bmatrix} -1 & -2\epsilon_{12} & 2\epsilon_{13} \\ 2\epsilon_{12} & -1 & 2\epsilon_{23} \\ -2\epsilon_{13} & -2\epsilon_{23} & -1 \end{bmatrix} .$$

The remaining reflection sequences are the reverse of the three sequences indicated in Eqs. (10) and (11). Their system reflection matrices may be obtained from the corresponding forward sequence matrices above by reversing the signs on the matrix elements in the upper right and lower left quadrants while leaving the main diagonal elements unchanged.

Once an illuminating beam $[S_0]$ is specified, we can now find the reflected beam vectors $[S]_{ijk}'$ for the corner cube by substituting each of our six system reflection matrices into Eq. (4). The prism is typically illuminated along its nominal axis of symmetry so that the aperture segments will have the same apparent size in the resulting interferogram. The $[S_0]$ direction cosines in this case are all equal to $\sqrt{3}/3$, and the correspond-

ing $[S]_{ijk}'$ components are

$$\begin{aligned} S'_{x_{123}} &= -\sqrt{3}/3(1 + 2\epsilon_{12} + 2\epsilon_{13}), \\ S'_{x_{213}} &= -\sqrt{3}/3(1 + 2\epsilon_{13} - 2\epsilon_{12}), \\ S'_{y_{123}} &= -\sqrt{3}/3(1 + 2\epsilon_{23} - 2\epsilon_{12}), \\ S'_{y_{213}} &= -\sqrt{3}/3(1 + 2\epsilon_{12} + 2\epsilon_{23}), \\ S'_{z_{123}} &= -\sqrt{3}/3(1 - 2\epsilon_{13} - 2\epsilon_{23}), \\ S'_{z_{213}} &= -\sqrt{3}/3(1 - 2\epsilon_{13} - 2\epsilon_{23}), \end{aligned} \quad (12)$$

and so on.

The six beams that emerge from the corner cube are interfered with a common reference beam to obtain a Twyman-Green interferogram. In order for the fringe patterns to be visually resolvable, their spatial frequencies must be low and the reference beam must in turn be nearly, but not exactly, coincident with the illuminating beam. This will guarantee that a small number of fringes will appear across the prism aperture even in the event that the prism is perfect. We can represent the direction cosines of such a reference vector $[0]$ as $[-(1/\sqrt{3}) + \delta_1, -(1/\sqrt{3}) + \delta_2, -(1/\sqrt{3}) + \delta_3]$. To first order, both the reference beam vector just mentioned and the emergent beam vectors, such as those given in Eq. (12), are of unit length. Hence the cross product between reference beam and emergent beam not only points in the direction that the fringes resulting from the interference of these two beams would have, but also has a magnitude equal to the sine of the angle between the two vectors. This magnitude is, of course, also equal to the wavelength of light times the spatial frequency of the fringes.

Using the two rays given in Eq. (12) we can show that

$$\begin{aligned} [S]_{123}' \times [0] &= \hat{i} [1/3(4\epsilon_{23} - 2\epsilon_{12} + 2\epsilon_{13}) - 1/\sqrt{3}(1 + 2\epsilon_{23} - 2\epsilon_{12})\delta_3 + 1/\sqrt{3}(1 - 2\epsilon_{13} - 2\epsilon_{23})\delta_2] \\ &+ \hat{j} [1/3(-2\epsilon_{23} - 2\epsilon_{12} - 4\epsilon_{13}) - 1/\sqrt{3}(1 - 2\epsilon_{13} - 2\epsilon_{23})\delta_1 + 1/\sqrt{3}(1 + 2\epsilon_{12} + 2\epsilon_{13})\delta_3] \\ &+ \hat{k} [1/3(-2\epsilon_{23} + 4\epsilon_{12} + 2\epsilon_{13}) - 1/\sqrt{3}(1 + 2\epsilon_{12} + 2\epsilon_{13})\delta_2 + 1/\sqrt{3}(1 + 2\epsilon_{23} - 2\epsilon_{12})\delta_1] \end{aligned} \quad (13)$$

and

$$\begin{aligned} [S]_{213}' \times [0] &= \hat{i} [1/3(4\epsilon_{23} + 2\epsilon_{12} + 2\epsilon_{13}) - 1/\sqrt{3}(1 + 2\epsilon_{23} + 2\epsilon_{12})\delta_3 + 1/\sqrt{3}(1 - 2\epsilon_{13} - 2\epsilon_{23})\delta_2] \\ &+ \hat{j} [1/3(-2\epsilon_{23} + 2\epsilon_{12} - 4\epsilon_{13}) - 1/\sqrt{3}(1 - 2\epsilon_{13} - 2\epsilon_{23})\delta_1 + 1/\sqrt{3}(1 - 2\epsilon_{12} + 2\epsilon_{13})\delta_3] \\ &+ \hat{k} [1/3(-2\epsilon_{23} - 4\epsilon_{12} + 2\epsilon_{13}) - 1/\sqrt{3}(1 - 2\epsilon_{12} + 2\epsilon_{13})\delta_2 + 1/\sqrt{3}(1 + 2\epsilon_{23} + 2\epsilon_{12})\delta_1]. \end{aligned} \quad (14)$$

These two fringe vectors, though complicated in form, differ only in the sign of their ϵ_{12} contributions. Subtracting Eq. (13) from (14) yields the difference vector

$$\begin{aligned} [S]_{213}' \times [0] - [S]_{123}' \times [0] &= (4/\sqrt{3})\epsilon_{12} [(1/\sqrt{3} - \delta_3)\hat{i} \\ &+ (1/\sqrt{3} - \delta_3)\hat{j} + (-2/\sqrt{3} + \delta_1 + \delta_2)\hat{k}]. \end{aligned} \quad (15)$$

If the quadratic factors in δ are neglected, the length of this resultant is given by

$$I_{\text{resultant}} = (4/\sqrt{3})\epsilon_{12} [2 - 4/\sqrt{3}(\delta_1 + \delta_2 + \delta_3)]^{1/2} . \quad (16)$$

By looking at the interference between the reference beam $[0]$ and the beam $[I]$ that would be reflected by a

perfect corner cube, we can evaluate the magnitude of the above $(\delta_1 + \delta_2 + \delta_3)$ factor

$$[I] \cdot [0] = 1 - 1/\sqrt{3}(\delta_1 + \delta_2 + \delta_3) = \cos \theta \approx 1 - \theta^2/2, \quad (17)$$

where θ = the angle between the two beams. The approximation given in the final step should be a good one since θ must be small for reasons given earlier. Equation (17) may be rearranged to get

$$\theta^2 = 2/\sqrt{3}(\delta_1 + \delta_2 + \delta_3) \quad (18)$$

or

$$(\delta_1 + \delta_2 + \delta_3) = \sqrt{3}/2 (\lambda F)^2, \quad (19)$$

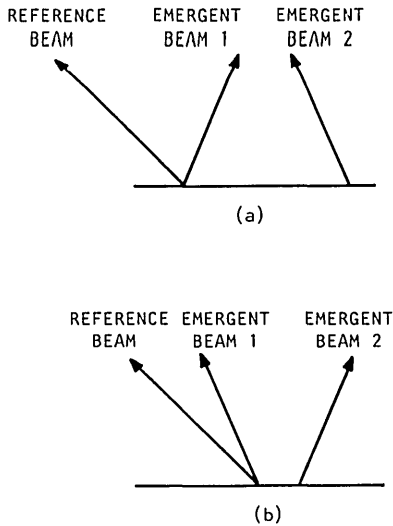


FIG. 2. Relative reference and emergent beam orientations that result in parallel fringe vectors. (a) Converging emergent beams. (b) Diverging emergent beams.

where F = the spatial frequency of the fringes that would be observed with a perfect corner cube. It should be noted that the fringe patterns associated with imperfect cubes will have spatial frequencies of the same order of magnitude as F since the various emergent beams make small angles with the illuminating beam in such cases provided the dihedral angle errors are small. Using Eq. (18) we can rewrite Eq. (16)

$$l_{\text{resultant}} = 4\sqrt{2/3} \epsilon_{12} [1 - (\lambda F)^2]^{1/2}. \quad (20)$$

For visible wavelengths and fringe spacings on the order of 1 mm or larger, $(\lambda F)^2$ is very small ($\sim 10^{-7}$) in comparison to unity, and we can say that, to a good approximation,

$$l_{\text{resultant}} = 4\sqrt{2/3} \epsilon_{12} \quad (21)$$

regardless of the particular reference beam used. If the above procedure is applied to $[S]_{231}$ and $[S]_{321}$, a difference vector magnitude of $4\sqrt{2/3} \epsilon_{23}$ is obtained while applying it to $[S]_{132}$, and $[S]_{312}$ yields a length of $4\sqrt{2/3} \epsilon_{13}$ for the difference vector.

It is of interest to note that the above three pairs of emergent beams correspond to the three pairs of prism aperture segments mentioned at the beginning of this section. The theory predicts that the magnitude of the dihedral angle error ϵ_{12} can be found by constructing vectors parallel to the fringes covering the aperture segments labeled "123" and "213" in Fig. 1 with lengths equal to the spatial frequencies of those fringes and then finding the length of the vector formed by subtracting one of these fringe vectors from the other. It also predicts that the magnitudes of ϵ_{13} and ϵ_{23} can be isolated using a similar analysis of the "132," "312" and "231," "321" pairs of fringe patterns, respectively.

The fringes that are recorded in a Twyman-Green interferogram are the projections of the actual fringes onto a plane that is nearly normal to the beam used to illuminate the corner cube. If the results obtained by the technique just described are to be accurate, we

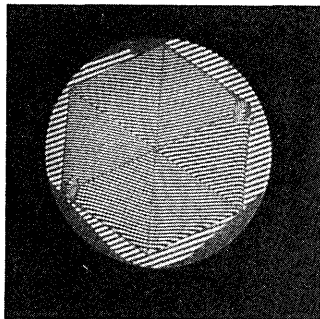
must be sure that the actual fringe vectors always lie sufficiently close to the interferogram plane to neglect their deviation from that plane. We know that if the beams reflected from the corner cube were interfered with a reference beam parallel to the beam used to illuminate the prism, the resulting fringes would all lie in the interferogram plane. We have shown that, for the reference beams that we expect to use, the angle between the reference and illuminating beams is equal to the product of the wavelength and fringe frequency, and that this product is on the order of 10^{-3} to 10^{-4} in magnitude. Thus for every case in which the assumptions we have already made concerning spatial frequencies of fringes are valid, the actual fringes should lie in planes that are sufficiently close to the interferogram plane for our above computational procedure to apply with good accuracy.

There is, of course, a problem involved in implementing this procedure experimentally. It is not obvious from examination of Twyman-Green interferograms what the directions of the associated fringe vectors should be. We can insure that the members of the above three pairs of fringe vectors both point in the same general direction for each pair by adjusting the reference beam prior to recording the interferogram so that it has an angular orientation outside that of the corresponding emergent beam vectors of each pair. Examples of this arrangement for vectors lying in one plane are illustrated in Fig. 2. Since the sense of rotation from the reference beam to each of the emergent beams in both of the cases shown in the figure is clockwise, the right-hand rule for determining the orientation of the cross product between two vectors predicts that the reference beam - emergent beam fringe vectors would all point into the plane of the paper in these examples. The above mentioned adjustment of the corner cube reference beam can normally be achieved in practice by selecting a reference mirror orientation that results in a large number of fringes over all the prism aperture segments. If the dihedral angle errors are all small, the emergent beams will make small angles with respect to one another so that reference beam orientations intermediate to any of the pairs of reflected beams being used to isolate these errors would result in low spatial frequency fringes over the corresponding pair of aperture segments. If the above precautions are taken in setting up a corner cube interferogram, the angles between the pairs of fringe vectors being used in the above subtraction process will always be given by the acute angles between the corresponding pairs of interferogram fringe patterns.

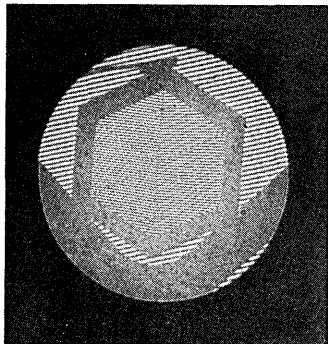
Finally, it should be noted that the ϵ_{ij} values calculated by the above technique should be divided by the refractive index to obtain the actual values when a glass prism is being tested interferometrically to compensate for refraction at the air-glass interface at the front of the corner cube.

EXPERIMENTAL VERIFICATION

Twyman-Green interferograms of a BK-7 glass corner cube and one consisting of front surface silvered



(a)



(b)

FIG. 3. Twyman-Green interferograms of two corner cubes. (a) BK-7 glass cube. (b) Front surface mirror cube.

mirrors are shown in Fig. 3. The fringe spacings and angular orientations of the fringe patterns in both interferograms were measured on a comparator. The acute angles between the pairs of fringe patterns needed to isolate the dihedral angle errors and the average spatial frequencies of all fringes were then calculated, and the results are given in Table I. The law of cosines was applied to the data in this table to find the lengths (in spatial frequency units) of the resultant vectors that were shown in the theory to be proportional to the dihedral angle errors. Finally, these errors (ϵ_{ij}) were computed from the difference vector lengths (L_{ij}) by means of the equation

$$\epsilon_{ij} = \lambda L_{ij} / 3.26mn \quad i=1, 2, \quad j=2, 3, \quad i \neq j. \quad (22)$$

The factor n stands for the prism index (1.514 for BK-7 or 1 for the mirror cube at $\lambda = 6563 \text{ \AA}$) and m stands for the ratio of the actual prism size to the interferogram

TABLE I. Comparator data for interferograms in Fig. 3.

Aperture segment	Glass cube		Mirror cube	
	Frequency (mm^{-1})	Relative angle (deg.)	Frequency (mm^{-1})	Relative angle (deg.)
213	1.92	3.72	1.99	0.55
123	1.61		1.87	
132	1.66	3.28	1.87	1.02
312	1.38		1.82	
321	1.63	18.54	1.92	5.25
231	1.62		1.91	

TABLE II. Dihedral angle error magnitudes for two corner cubes.

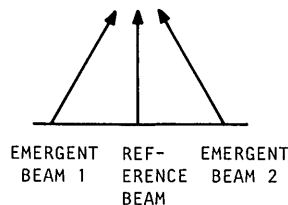
	Glass cube		Mirror cube	
	Computed value (arc sec)	Goniometer value (arc sec)	Computed value (arc sec)	Goniometer value (arc sec)
ϵ_{12}	7.59	-6.13	4.26	-3.35
ϵ_{13}	6.74	7.90	2.13	3.27
ϵ_{23}	12.03	-11.67	6.23	-5.25

size. This magnification factor is necessary because the fringe frequencies and the value of L , which is calculated in terms of them, depend on interferogram size and so must be corrected to the size of the prism. In our case, the values of m were 1.16 and 1.14 for the glass and mirror cubes, respectively. The computed errors are given in Table II for both corner cubes and are estimated to be accurate to within ± 1 arc sec. The primary cause for variation in the computed ϵ values about the average values given in the table was variation in the comparator line spacing measurements within a single fringe pattern. This variation was greatest for the BK-7 cube data and was due largely to fringe curvature caused by deviation in the prism reflecting surfaces from flatness.

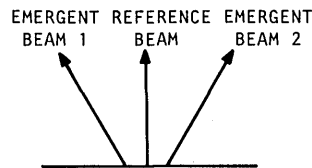
The dihedral angles in both corner cubes were also externally measured one at a time with a goniometer. These values are given in Table II and were also repeatable to within about ± 1 arc sec. It was, of course, possible to recover the signs as well as the magnitudes of the errors with the goniometer. Comparison of the corresponding error magnitudes obtained by the two methods shows agreement to within the accuracies of the measurements.

CONCLUSION

The procedure presented in this paper for recovering the magnitudes of the dihedral angle errors in a corner



(a)



(b)

FIG. 4. Relative reference and emergent beam orientations that result in parallel fringes of equal spatial frequency. (a) Converging emergent beams. (b) Diverging emergent beams.

cube from its Twyman-Green interferogram is convenient and apparently accurate. In the absence of additional information, it is, however, impossible to recover the signs of these errors from a single interferogram. A technique often used in interferometry to obtain information concerning the signs of errors is to adjust the tilt of the reference beam after the interferogram has been recorded and observe the resulting changes in the fringe patterns. For example, if the reference beam were oriented by appropriate adjustment of the interferometer reference mirror so as to give fringes of equal spatial frequency over one of the pairs of aperture segments being used to evaluate one of the dihedral angle errors, the corresponding beam orientations would be as shown in Fig. 4. A further clockwise rotation of the reference beam from the posi-

tion shown in the figure would result in an increase in the spatial frequency of the fringes resulting from the interference of the right-hand pair of beams if the emergent beams were converging ($\epsilon < 0$) and a decrease if they were diverging ($\epsilon > 0$). The same procedure applied to the other two pairs of fringe patterns would also give the signs of their associated dihedral angle errors.

¹P. R. Yoder, Jr., "Study of light deviation errors in triple mirrors and tetrahedral prisms," *J. Opt. Soc. Am.* 48, 496-499 (1958).

²Bernard W. Joseph and Robert J. Donohue, "Dot patterns from imperfect cube-corner reflectors," *J. Opt. Soc. Am.* 62, 727 (1972).

³Military Standardization Handbook 141, Defense Supply Agency, Washington, D.C., 13-1 through 13-9.

Seventh spectrum of selenium: Se_{VII} and the $3p^5 3d^{10}$ configuration in Se_{VIII}

Th. A. M. van Kleef

Zeeman Laboratorium, Universiteit van Amsterdam, Amsterdam, The Netherlands

Y. N. Joshi

Physics Department, St. Francis Xavier University, Antigonish, Nova Scotia, Canada B2G 1C0

(Received 7 August 1976)

The spectrum of selenium has been observed in the wavelength region 1200-100 Å on the 10.7 m normal incidence and 10.7 m grazing incidence vacuum spectrographs at the NBS Laboratory in Washington. A triggered vacuum spark was used as a source. The "pole effect" exhibited by the lines on the normal incidence spectrograms helped to discriminate different stages of ionization of the selenium spectra. All the levels belonging to the $3d^9 4s$ and $3d^9 4p$ configurations in Se_{VII} have been located. The parametric level fitting calculations of the energy levels agree with the experimental values. In Se_{VIII} , the $3p^5 3d^{10} 2P^\circ$ term has been determined.

INTRODUCTION AND EXPERIMENTAL

The six-times ionized selenium atom Se_{VII} is isoelectronic with Ni_{I} . Its ground state configuration is $3d^{10} 1S_0$ and the first two excited configurations are $3d^9 4s$ and $3d^9 4p$. In 1934 Kruger and Shoupp¹ observed four lines in the region 170-180 Å and classified three of them as transitions between $3d^{10} 1S_0$ and $3d^9 4p^3 P_1^\circ$, $1P_1^\circ$ and $3D_1^\circ$, on the basis of the extrapolations in the Ni_{I} isoelectronic sequence. In the same year Rao and Murti² published a list of 44 lines in the region 561-860 Å, out of which they assigned 42 lines to the Se_{VII} spectrum. They also suggested the classifications for four of these lines. Edlén³ classified many lines below 113 Å as transitions to the ground state level from levels of the $3d^9 5p$ and $3d^9 nf$ ($n=4$ to 8) configurations. Recently we published revised values⁴ for the resonance lines of Se_{VII} . From Ni_{I} isoelectronic sequence extrapolation the transitions belonging to $3d^9 4s - 3d^9 4p$ may be predicted to fall in the region 700-950 Å.

The spectrum of selenium was photographed in the region 525-1220 Å on the 10.7 m normal incidence spectrograph in the NBS Laboratory in Washington. This supplemented our earlier observations⁴ below 600 Å on the 10.7 m grazing incidence spectrograph. The

source used was a triggered vacuum spark as described by Feldman *et al.*⁵ Spectroscopically pure selenium was packed into an axial cavity of an aluminum electrode which was used as a cathode. The anode was a pure aluminum electrode. Aluminum has very few lines in the wavelength region studied and only the strongest ones appeared on our plates. The electrode separation was about 3 mm. The charging potential was varied from 5 to 12 kV and the conditions of the discharge were controlled further by inserting induction coils in the circuit. By comparing the intensities of the lines under different experimental conditions, the ionization stages could be determined quite definitely. Since the spectrograph was stigmatic, the lines showed a pole effect⁶ of varying degree for the lines of different ionization stages. The lines belonging to Se_{II} , Se_{III} , Se_{IV} , and Se_{V} did not show any pole effect. The intensity of Se_{VI} lines tapered off from the top to the bottom along the length of the lines, while for the Se_{VII} lines the tapering-off effect was much more enhanced. Se_{VIII} lines appeared only as tips (about $\frac{3}{4}$ to $\frac{1}{4}$ of the length of the line at 10 kV and shorter at lower voltages) and did not appear on 5 kV exposures. This is shown in Fig. 1. Thus the pole effect provided a very reliable means to discriminate various higher ionization stages of the